

CCA-1207

YU ISSN 0011-1643

UDC 541.183:54—31

Conference Paper

A Ligand Exchange Model for the Adsorption of Inorganic and Organic Ligands at Hydrus Oxide Interfaces*

Werner Stumm, Robert Kummert, and Laura Sigg

Institute of Aquatic Sciences (EAWAG),
Swiss Federal Institute of Technology (ETH), Zürich, Switzerland

Received September 24, 1979

Specific adsorption of organic and inorganic weak acids and of anions on hydrus oxide surfaces and the concomitant influences upon surface charge can be interpreted as ligand exchange reactions at the reactive surface sites. Direct (inner sphere) binding of the ligands to the surface is postulated. The extent of adsorption and its pH dependence can be explained by considering the affinity of the surface sites and those of the ligands. Surface equilibrium constants have been determined experimentally for various surface reactions; they can be used to predict extent of adsorption and resulting surface charge. The adsorption of simple weak acids or their anions is largest around the pH value of $\text{pH} = \text{pK}$. The surface complex formation constants show the same trend in stability as the corresponding solute complex formation constants; thus surface coordination equilibrium constants can be estimated from the corresponding complex formation constants in solution.

INTRODUCTION

Oxides especially those of Si, Al and Fe are abundant components of the earth crust. Interaction of cations, weak acids and anions with hydrus oxide surfaces are of importance in colloid chemistry in natural water systems and in geochemical processes. In the presence of water the surfaces of metal or metalloid oxides are generally covered with surface hydroxyl groups (Figure 1). The pH-dependent charge of a hydrus oxide results from proton transfers at the surface.

Surface coordination. Thus, a hydroxylated oxide particle can be treated like a polymeric oxo acid (or base) and the »specific adsorption« of H^+ , OH^- and of cations and anions can be interpreted in terms of coordination reactions at the oxide water interface (Figure 2). The interfacial coordination chemistry of hydrus oxides with respect to cations (metal ions) has been treated before². The specific** adsorption of anions and their conjugate acids to oxide surfaces can be interpreted in terms of a ligand exchange where the structural metal ion replaces its coordinative ligand OH^- by another ligand³.

* Based on an invited lecture presented at the 5th »Ruder Bošković« Institute's International Summer Conference *Chemistry of Solid/Liquid Interfaces*, Cavtat/Dubrovnik, Croatia, Yugoslavia, June 1979.

** Specific adsorption occurs if binding mechanisms, other than coulombic ones are significantly involved.

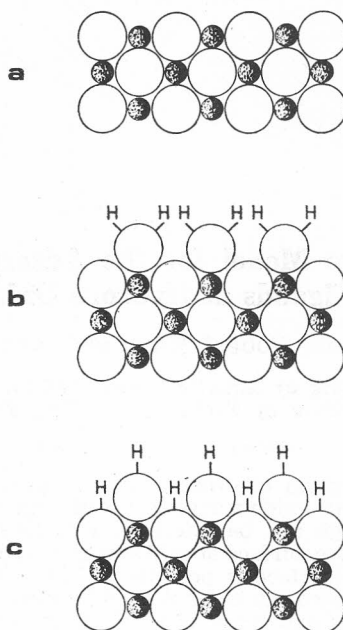


Figure 1. Schematic View of a Cross Section of the Surface Layer of a Metal Oxide (from P. W. Schindler¹). The metal ions in the surface layer behave as Lewis acids. In the presence of water the surface metal ions tend to coordinate H_2O molecules (Figure 1a, b). For most of the oxides dissociative chemisorption of water molecules (Figure 1c) seems energetically favoured.

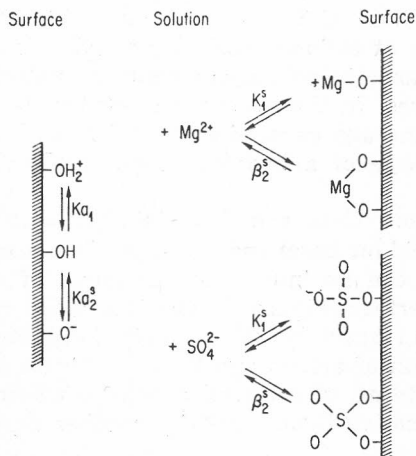


Figure 2. Interaction of Hydrous Oxides with Acid and Base and with Cations and Anions, exemplified for the specific adsorption of Mg^{2+} and SO_4^{2-} , is interpreted in terms of surface complex formation and ligand exchange equilibria. The surface coordination equilibria are given in Eqs. (1–6).

The interaction of reactive surface sites with solutes (that can be coordinated to these sites) is expressed in terms of an equilibrium mass law; the interaction is characterized by a materials' balance and a particular free energy change.

The objectives of this paper are:

(1) to illustrate that the specific adsorption of anions and weak acids on hydrous oxide surfaces can be quantitatively interpreted as a ligand exchange equilibrium and that one can predict with the equilibrium constants of the surface coordination reactions the extent of specific anion adsorption and the surface charge and their dependence on pH and other solution variables;

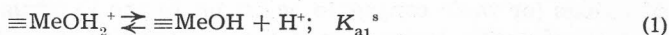
(2) to show that the tendency of ligands to form surface complexes at the oxide-water interface is comparable to that to form corresponding metal complexes in solution and to present other evidence indicating that the specifically adsorbed ligands might be viewed as »inner sphere« complexes;

(3) to compare briefly the equilibrium surface coordination model with an electric double layer model and to discuss the difficulties involved in attempting to separate the chemical and electrostatic energy of the surface coordination reaction; and

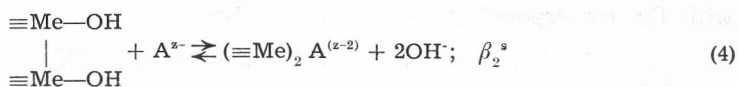
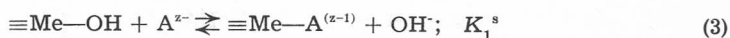
(4) to describe the experimental approach that may be used to assess the extent of surface coordination and surface charge and to evaluate surface coordination equilibrium constants.

THE LIGAND EXCHANGE MODEL

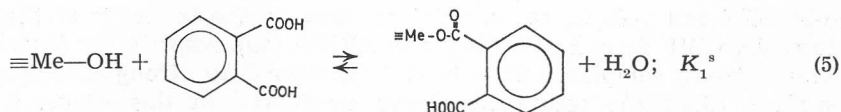
The metal ion in the surface layer, acting as a Lewis acid, exchanges the general ligand OH^- against an other Lewis base. In addition to the acid-base reactions of the surface



some of the postulated ligand exchange reactions are



or



For protonated anions the ligand exchange may be accompanied by a deprotonation of the ligand at the surface. For example, in the case of HPO_4^{2-} :



The tendency of solutes to interact with the surface sites can be expressed quantitatively in terms of equilibrium constants, such as

$$K_{a1}^s = \frac{\{\equiv\text{MeOH}\} [\text{H}^+]}{\{\equiv\text{MeOH}_2^+\}}; K_1^s = \frac{\{\equiv\text{MeA}^{(q-1)}\} [\text{OH}^-]}{\{\equiv\text{MeOH}\} [\text{A}^{q-}]}; \beta_2^s = \frac{\{\equiv\text{Me}_2\text{A}^{(q-2)}\} [\text{OH}^-]^2}{\{\equiv\text{Me}_2\text{OH}_2\} [\text{A}^{q-}]}$$

where $\{\}$ and $[\]$ indicate, respectively, concentrations of surface species, (e. g. mol kg⁻¹)^{*} and of solutes (M) N at equilibrium. As Equation (4) illustrates, under certain circumstances bidentate complexes (cf. Figure 2) may be formed. This may depend on the steric compatibility; e. g., the distance between OH⁻ groups of goethite and the O—O distance of a phosphate ion are of similar size, while the binding of one aromatic dicarboxylic acid to two surface groups of $\gamma\text{-Al}_2\text{O}_3$ is unlikely for geometric reasons.

The equilibrium constants are valid for a given ionic strength and depend on the surface charge. The free energy of deprotonation of reaction (1) consists of the dissociation as measured by an intrinsic acidity constant, K_a^s (intr.) and the removal of the proton from the site of the dissociation into the bulk of the solution as expressed by the Boltzman factor; thus

$$K_1^s = K_1^* \text{ (intr.) } \exp (F\psi_s/RT) \quad (7)$$

where ψ_s is the effective potential difference between the surface site and the bulk solution; K_a^s (intr.) is the acidity constant of an acid group in a hypothetically completely chargeless surrounding. There is no direct way to obtain ψ_s theoretically or experimentally. It is possible, however, to determine the microscopic constants experimentally and to extrapolate these constants to zero surface charge in order to obtain intrinsic constants; equilibrium constants determined for goethite^{4,5} and for $\gamma\text{-Al}_2\text{O}_3$ ^{6,7} are quoted in Table I.

Comparable Tendency of Ligands to Form Complexes in Solution as at the Oxide-Water Interface. We are justified to interpret the specific adsorption of anions (or their conjugate acids) on to the hydrous oxide surface in terms of a coordinative interaction if the tendency of various ligands to form metal complexes in solution is similar to that of specific adsorption at the surface of the corresponding hydrous metal oxide. We may for example compare the surface coordination of the acid H₂A



with the corresponding reaction in solution



Comparable equation can be written for the interaction with monoprotic acids. Figure 3 illustrates that the tendency of ligands to replace OH⁻ from $\alpha\text{-FeOOH}$ and $\gamma\text{-Al}_2\text{O}_3$ surfaces is the same as the tendency of these ligands to replace OH⁻ from FeOH²⁺ (aq) and AlOH²⁺ (aq), respectively (equations 8, 9). Thus, strong complexes in solution correspond to strong complexes at the surface. Since the solute complexes considered in this Figure are »inner sphere« complexes, we may infer that the surface complexes formed are of the inner sphere type.

* Other units ([mol m⁻²] or [mol dm⁻³]) for a given concentration of dispersed oxides may be used, because these concentrations cancel in the mass law expressions.

TABLE I

Coordination of α -FeOOH (Goethite) and γ -Al₂O₃ with Anions or Their Conjugate Acids

	Intrinsic constant (22 °C)* log K
1. Goethite (from ref. 4)	
$\equiv\text{FeOH}_2^+ \rightleftharpoons \equiv\text{FeOH} + \text{H}^+$	— 6.4
$\equiv\text{FeOH} \rightleftharpoons \equiv\text{FeO}^- + \text{H}^+$	— 9.25
$\equiv\text{FeOH} + \text{F}^- \rightleftharpoons \equiv\text{FeF} + \text{OH}^-$	— 4.8
$\equiv\text{FeOH} + \text{SO}_4^{2-} \rightleftharpoons \equiv\text{FeSO}_4^- + \text{OH}^-$	— 5.8
$2\equiv\text{FeOH} + \text{SO}_4^{2-} \rightleftharpoons \equiv\text{Fe}_2\text{SO}_4 + 2\text{OH}^-$	—13.5
$\equiv\text{FeOH} + \text{HAc} \rightleftharpoons \equiv\text{FeAc} + \text{H}_2\text{O}$	2.9
$\equiv\text{FeOH} + \text{H}_4\text{SiO}_4 \rightleftharpoons \equiv\text{FeSiO}_4\text{H}_3 + \text{H}_2\text{O}$	4.1
$\equiv\text{FeOH} + \text{H}_4\text{SiO}_4 \rightleftharpoons \equiv\text{FeSiO}_4\text{H}_2^- + \text{H}_3\text{O}^+$	— 3.3
$\equiv\text{FeOH} + \text{H}_3\text{PO}_4 \rightleftharpoons \equiv\text{FePO}_4\text{H}_2 + \text{H}_2\text{O}$	9.5
$\equiv\text{FeOH} + \text{H}_3\text{PO}_4 \rightleftharpoons \equiv\text{FePO}_4\text{H}^- + \text{H}_3\text{O}^+$	5.1
$\equiv\text{FeOH} + \text{H}_3\text{PO}_4 \rightleftharpoons \equiv\text{FePO}_4^{2-} + 2\text{H}^+ + \text{H}_2\text{O}$	— 1.5
$2\equiv\text{FeOH} + \text{H}_3\text{PO}_4 \rightleftharpoons \equiv\text{Fe}_2\text{PO}_4\text{H} + 2\text{H}_2\text{O}$	8.5**
$2\equiv\text{FeOH} + \text{H}_3\text{PO}_4 \rightleftharpoons \equiv\text{Fe}_2\text{PO}_4^- + \text{H}^+ + 2\text{H}_2\text{O}$	4.5
2. γ-Al₂O₃ (from ref. 6)	
	log K
$\equiv\text{AlOH}_2^+ \rightleftharpoons \equiv\text{AlOH} + \text{H}^+$	— 7.4
$\equiv\text{AlOH} \rightleftharpoons \equiv\text{AlO}^- + \text{H}^+$	—10.0
Benzoic acid	
$\equiv\text{AlOH} + \text{HA} \rightleftharpoons \equiv\text{AlA} + \text{H}_2\text{O}$	3.7 ± 0.3
Catechol	
$\equiv\text{AlOH} + \text{H}_2\text{A} \rightleftharpoons \equiv\text{AlA}^- + \text{H}_3\text{O}^+$	3.7 ± 0.3
$\equiv\text{AlOH} + \text{H}_2\text{A} \rightleftharpoons \equiv\text{AlA}^- + \text{H}_3\text{O}^+$	< -5
Phthalic acid	
$\equiv\text{AlOH} + \text{H}_2\text{A} \rightleftharpoons \equiv\text{AlAH} + \text{H}_2\text{O}$	7.3 ± 0.3
$\equiv\text{AlOH} + \text{H}_2\text{A} \rightleftharpoons \equiv\text{AlA}^- + \text{H}_3\text{O}^+$	2.4 ± 0.4
Salicylic acid	
$\equiv\text{AlOH} + \text{H}_2\text{A} \rightleftharpoons \equiv\text{AlAH} + \text{H}_2\text{O}$	6.0 ± 0.4
$\equiv\text{AlOH} + \text{H}_2\text{A} \rightleftharpoons \equiv\text{AlA}^- + \text{H}_3\text{O}^+$	—0.6 ± 0.6

* Equilibrium constants are defined as:

$$K_{a1}^s = \frac{[\equiv\text{FeOH}][\text{H}^+]}{[\equiv\text{FeOH}_2^+]}$$

All concentrations are given in mol dm⁻³

** Bidentate equilibria are defined as:

$$K = \frac{[\equiv\text{Fe}_2\text{PO}_4\text{H}]}{[\equiv\text{FeOH}][\text{H}_3\text{PO}_4]}$$

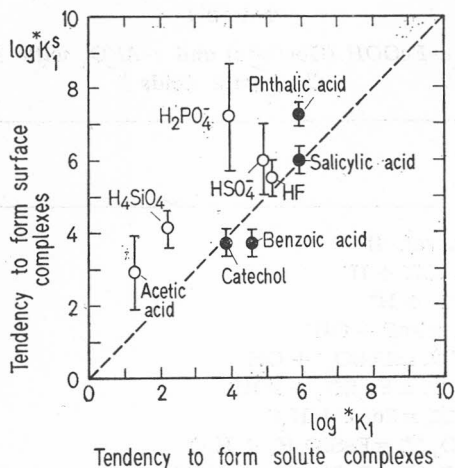


Figure 3. Comparison of the Tendency to form Surface Complexes ($*K_1^s$, Eq. 8) with that to form solute complexes ($*K_1$, Eq. 9)

- (O) with α -FeOOH and FeOH^{2+} , respectively;
 (●) with γ - Al_2O_3 and AlOH^{2+} , respectively.

Enhancement of the Acidity of Surface Complexes. If a surface coordinated acidic ligand is not separated from the structural surface metal ion by one or more water molecules, the surface should enhance significantly the acidity of the surface bound acidic ligands. This is indeed the case as will be illustrated by comparing the acidity constants of surface species with those of comparable solute species (Table II). The acidification induced by the proximity of the structural metal ion in the surface is significant; it is however not as large as that caused by an aquo Fe(III) or aquo Al(III) ion because the charge of the Fe(III) or Al(III) in the surface (where these atoms are already coordinated to other O-ions) is not exerted to the same extent as in the soluble complex.

EXPERIMENTAL EVALUATION OF SURFACE COORDINATION EQUILIBRIUM CONSTANTS, SURFACE CHARGE AND SURFACE SPECIATION

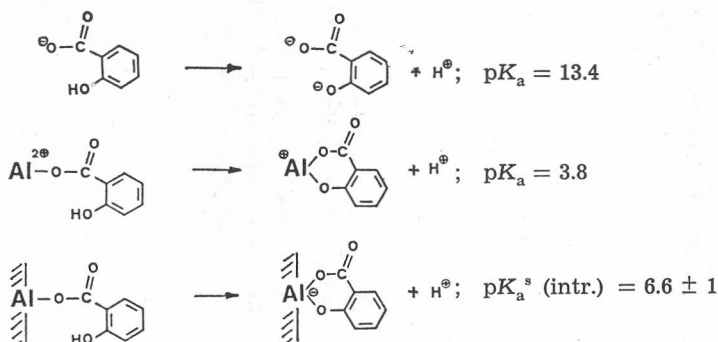
Based on the arguments given above, we imply that adsorbed ligands are bound directly to the structural metal ions of the oxide surface. The charge of these ions can thus be assigned to the same plane as the charges caused by proton transfer of the surface-OH groups. We have used essentially the same experimental approach as that used for the evaluation of solute ligand exchange equilibria, or more specifically for equilibria with polymeric oxo acids and bases. All measurements were made in the presence of a constant ionic medium of indifferent (not specifically adsorbable) electrolytes (10^{-1} M or 10^{-2} M NaClO_4).

The *extent of adsorption* (surface coordination) and the *surface charge* were determined as a function of pH and other solution variables and surface area concentration in order to determine (1) the surface coordination equilibrium constants, (2) their dependence upon surface charge, and (3) the type of surface species formed (e. g., monodentate or bidentate complex, protonated or deprotonated surface ligand). For each oxide surface the concentration of surface sites (exchange capacity),

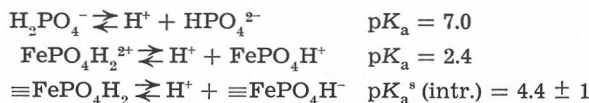
TABLE II

Enhancement of the Acidity of Surface Coordinated Acidic Ligands

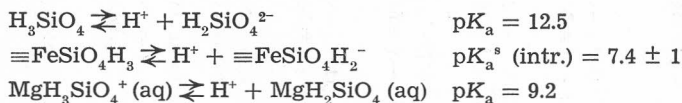
1. Comparisons of the second acidity constant of salicylic acid with the acidity constant of salicylato-Al(III) (aq) and of the γ -Al₂O₃-surface coordinated salicylate [from refs. 6, 7]



2. Comparison of the acidity constant of H₂PO₄⁻ with that of FePO₄H₂²⁺ (aq) and of α -FeOOH-coordinated H₂PO₄⁻ [from refs. 4, 5]



3. Comparison of the acidity constant of H₃SiO₄⁻ with that of α -FeOOH bound H₃SiO₄⁻ and that of MgH₃SiO₄⁺ (aq) [from 4, 5]



$$\begin{aligned}
 \{\equiv\text{MeOH}_T\} &= \{\equiv\text{MeOH}_2^+\} + \{\equiv\text{MeOH}\} + \{\equiv\text{MeO}^-\} + \\
 &+ \Sigma \{\equiv\text{MeOM}\} + \Sigma \{\equiv\text{MeA}\}
 \end{aligned} \quad (10)$$

is determined experimentally. In some instances, the electrokinetic potential ζ from which the electrokinetic charge can be estimated, was determined.

The extent of adsorption was measured analytically, usually from charges in solute concentrations after attaining »equilibrium«. Equilibration periods of 1—2 days were allowed. Alkalimetric or acidimetric titration curves in presence and absence of specifically adsorbable ligands permit to determine (i) the extent of ligand adsorption (if the type of surface species formed is known (Table III)) and (ii) the surface charge. Knowing the (analytically determined) extent of adsorption and the surface charge (from titration curves) as a function of pH and other solution variables permits to deduce the type of surface species formed.

The alkalimetric or acidimetric titration curves obtained in the absence of specifically adsorbable species permit to determine that portion of the

TABLE III
Alkalimetric and Acidimetric Titration of Hydrrous Oxide

	Charge Balance	Shift of titration curve at constant pH $\Delta c = (c_A^* - c_B^* - (c_A - c_B))$
No specific adsorption	$(c_B - c_A + [H^+] - [OH^-]) \cdot 1/a = \{ \equiv \text{MeO} \} - \{ \equiv \text{MeOH}_2^+ \}$	
Specific adsorption of M^{2+}	$(c_B^* - c_A^* + [H^+] - [OH^-] + 2[M^{2+}] - 2[M^{2+}]_T) \cdot 1/a = \{ \equiv \text{MeO} \}^* - \{ \equiv \text{MeOH}^+ \}$	$\Delta c \cdot 1/a = -(2\alpha_0 + \alpha_1) \{ \equiv \text{MeOM}^+ \} + 2 \{ \equiv \text{MeO} \}_2 M$
Specific adsorption of A^{2-}	$(c_B^* - c_A^* + [H^+] - [OH^-] - 2[A^{2-}] + 2[A^{2-}]_T) \cdot 1/a = \{ \equiv \text{MeO} \}^* - \{ \equiv \text{MeOH}_2^+ \} + \{ \equiv \text{MeA}^- \}$	$\Delta c \cdot 1/a = (\alpha_1 + 2\alpha_2) \{ \equiv \text{MeA}^- \} + 2 \{ \equiv \text{Me}_2\text{A} \}$
Specific adsorption of HA	$(c_B^* - c_A^* + [H^+] - [OH^-] - [A^-]) \cdot 1/a = \{ \equiv \text{MeO} \}^* - \{ \equiv \text{MeOH}_2^+ \} - \{ \equiv \text{Me}_2\text{A}^+ \}$	$(\Delta c + [\text{HA}_T] - [\text{HA}]) \cdot 1/a = (\alpha_1 + 2\alpha_2) \{ \equiv \text{MeA} \} + 2 \{ \equiv \text{Me}_2\text{A}^+ \}$
Specific adsorption of H_2A	$(c_B^* - c_A^* + [H^+] - [OH^-] - [\text{HA}] - 2[A^{2-}]) \cdot 1/a = \{ \equiv \text{MeO} \}^* - \{ \equiv \text{MeOH}_2^+ \} + \{ \equiv \text{MeA} \}$	$(\Delta c + [\text{HA}_T] + 2[A^{2-}]) \cdot 1/a = (\alpha_2 - \alpha_1) \{ \equiv \text{MeAH} \} + \{ \equiv \text{MeA}^- \} + 2 \{ \equiv \text{Me}_2\text{A} \} - \{ \equiv \text{MeA}^- \}$

A^{2-} means an anion not protonated in the pH range of titrations.

c_A, c_B : concentrations of strong acid and strong base [mol dm⁻³].

a : quantity of oxide used [kg dm⁻³].

*: concentrations in presence of specifically adsorbable ions.

$$\alpha_0 = \frac{\{ \equiv \text{MeOH}_2^+ \}}{\{ \equiv \text{MeOH}_T \}} \quad \alpha_1 = \frac{\{ \equiv \text{MeOH} \}}{\{ \equiv \text{MeOH}_T \}} \quad \alpha_2 = \frac{\{ \equiv \text{MeO} \}}{\{ \equiv \text{MeOH}_T \}}$$

$\alpha_1 = \alpha_1^*$ at constant pH.

It is assumed that the proportion of protonated to non protonated free surface groups is not affected by adsorption at constant pH.

charge, Q (moles per kg), which is due to H^+ or OH^- on the basis of the proton condition (or charge balance)

$$Q = \{\equiv MeOH_2^+\} - \{\equiv MeO^-\} = (c_A - c_B + [OH^-] - [H^+])/a \quad (11)$$

where c_B and c_A are concentrations (in $mol\ dm^{-3}$) of a strong base and strong acid added, respectively; a is the quantity of oxide used ($kg\ dm^{-3}$). The corresponding surface charge σ_o ($C\ m^{-2}$) is given by $\sigma_o = QF/S$, where S is the specific surface area ($m^2\ kg^{-1}$) and F is the Faraday constant ($C\ mol^{-1}$). With the help of these titration curves the acidity of the $\equiv MeOH$ groups and the pH of zero proton condition, pH_{zpc} , can be determined. In presence of specifically adsorbable ions, the surface charge is established by the proton balance at the surface (binding of H^+ or OH^- and their complexes) and specifically bound cations and anions:

$$\sigma_o = F (\Gamma_H - \Gamma_{OH^-} + \sum_i z \Gamma_{M_i^{z+}} - \sum_i z \Gamma_{A_i^{z-}}) \quad (12)$$

where F = Faraday constant ($C\ mol^{-1}$), z = magnitude of the charge of the non-hydrolyzed cation or deprotonated anion, Γ_H , Γ_{OH^-} and $\Gamma_{M^{z+}}$, $\Gamma_{A^{z-}}$ are the adsorption densities ($mol\ m^{-2}$) of H^+ (and its complexes) of OH^- (and its complexes), of cations and of the deprotonated anion, respectively.

σ_o is accessible from the titration curve which always reflects a charge balance; in case of an adsorbable anion ligand A^{z-}

$$\begin{aligned} Q &= \frac{\sigma_o S}{F} = c_A - c_B + [OH^-] - [H^+] + z ([A^{z-}] - [A_T^{z-}]) = \\ &= \{\equiv MeOH_2^+\} - \{\equiv MeO^-\} - \sum z \{\equiv MeA^{z-}\} \end{aligned} \quad (13)$$

Exemplifications

The principles involved will be illustrated by treating in some detail (1) the determination of the acidity constant of α -FeOOH; (2) the surface coordination of F^- on α -FeOOH; and (3) the surface coordination of phthalic acid on γ - Al_2O_3 .

Amphoteric Properties of α -FeOOH. Figure 4 (from ref. 4) gives the alkalimetric titration curve (Figure a) and the surface charge as a function of pH (b). At pH values below and above pH_{zpc} ($Q = 0$) the following approximations are justified:

$$\begin{aligned} pH < pH_{zpc} : \{\equiv FeOH_2^+\} &> \{\equiv FeO^-\}; \\ \{\equiv FeOH_2^+\} &= Q; \\ \{\equiv FeOH\} &= \{\equiv FeOH_T\} - Q, \end{aligned} \quad (14)$$

and

$$\begin{aligned} pH > pH_{zpc} : \{\equiv FeO^-\} &= -Q \\ \{\equiv FeOH_2^+\} &= \{\equiv FeOH_T\} + Q \end{aligned} \quad (15)$$

As Figure 4 c shows the microscopic acidity constants pK_{a1}^s and pK_{a2}^s are approximated as linear functions of Q and intrinsic constants can be obtained by extrapolation to $Q = 0$:

$$pK_{a1}^s = pK_{a1}^s(\text{intr}) - bQ \quad (16)$$

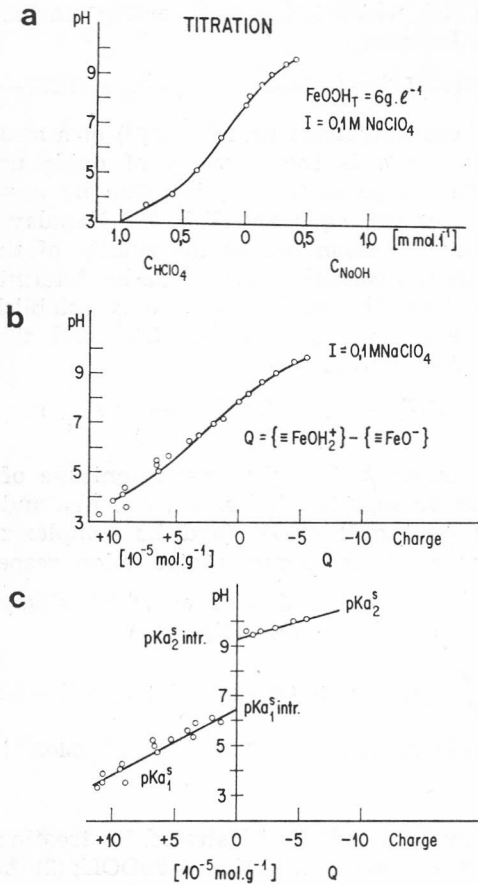


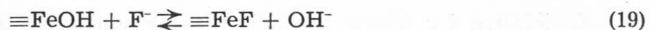
Figure 4. Alkalimetric/Acidimetric Titration Curve (Figure 4a) and the Surface Charge of Goethite as a Function of pH, calculated with Eq. (11) (Figure 4b). Microscopic acidity constants of goethite as a linear function of the charge (Figure 4c).

$$pK_{a_2}^s = pK_{a_2}^s(\text{intr}) + b'Q \quad (17)$$

Comparing equations (16), (17) with equation (7) shows that the differential capacity of the double layer $C = \sigma_o/\psi_s$, possibly as a consequence of the relatively high ionic strength of the solution, is constant. The point of zero proton condition (zero point of charge) is given by

$$pH_{zpc} = 1/2 [pK_{a_1}^s(\text{intr}) + pK_{a_2}^s(\text{intr})] \quad (18)$$

Surface Coordination of F⁻ on α-FeOOH. Figure 5 (from ref. 4) gives alkalimetric titration curves of α-FeOOH in absence and presence of F⁻. The displacement of the curve and its extent is caused by the reaction



The surface charge in absence and presence of F⁻ (Figure 5b) is given respectively by (cf. Table III)

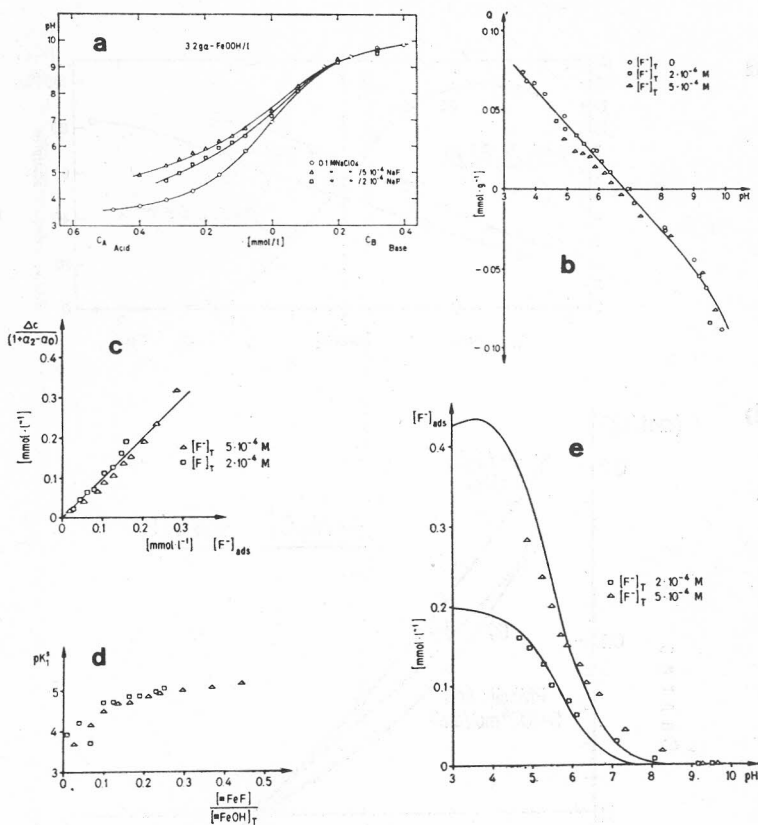


Figure 5. Adsorption of F^- on Goethite. The specific adsorption (surface coordination) of F^- causes a displacement of the titration curve for α -FeOOH (Figure 5a) from which the extent of adsorption and the resulting surface charge can be calculated (Figure 5b). The displacement of the titration curve (corrected for protolysis) versus the concentration of F^- adsorbed is plotted in Figure 5c (cf. Table III). The slope of 1 indicates that monodentate surface complexes only are formed. The equilibrium constants can be plotted as a function of the degree of loading (Figure 5d). The extent of specific adsorption of F^- on α -FeOOH is plotted in Figure 5e. Lines were calculated from the experimentally determined equilibrium constant (eq. (3), Table I). Points are experimental.

$$Q = 1/a (c_A - c_B - [H^+] + [OH^-]) = 1/a (\{ \equiv FeOH_2^+ \} - \{ \equiv FeO^- \}) \quad (20)$$

$$Q^* = 1/a (c_A^* - c_B^* - [H^+] + [OH^-] + [F^-] - [F_T^-]) = \\ = 1/a (\{ \equiv FeOH_2^+ \}^* - \{ \equiv FeO^- \}^*) \quad (21)$$

In exchanging OH^- against F^- no charged groups are formed, but $\equiv FeF$ is no longer available for protonation or deprotonation; thus only a shift change in the charge vs pH (Figure 5b) results. A plot of $\Delta c / (a_1 + 2a_2)$ vs F^- bound (cf. Table III) gives a slope of 1 indicating that only monodentate F^- complexes are formed on the surface (Figure 5c). The equilibrium constants calculated from the experimental data are plotted as a function of the degree of loading ($\{ \equiv FeF \} / \{ \equiv Fe_T \}$) in Figure 5d. Obviously the equilibrium constants show marked variation which may be caused by variations in activity coefficients of

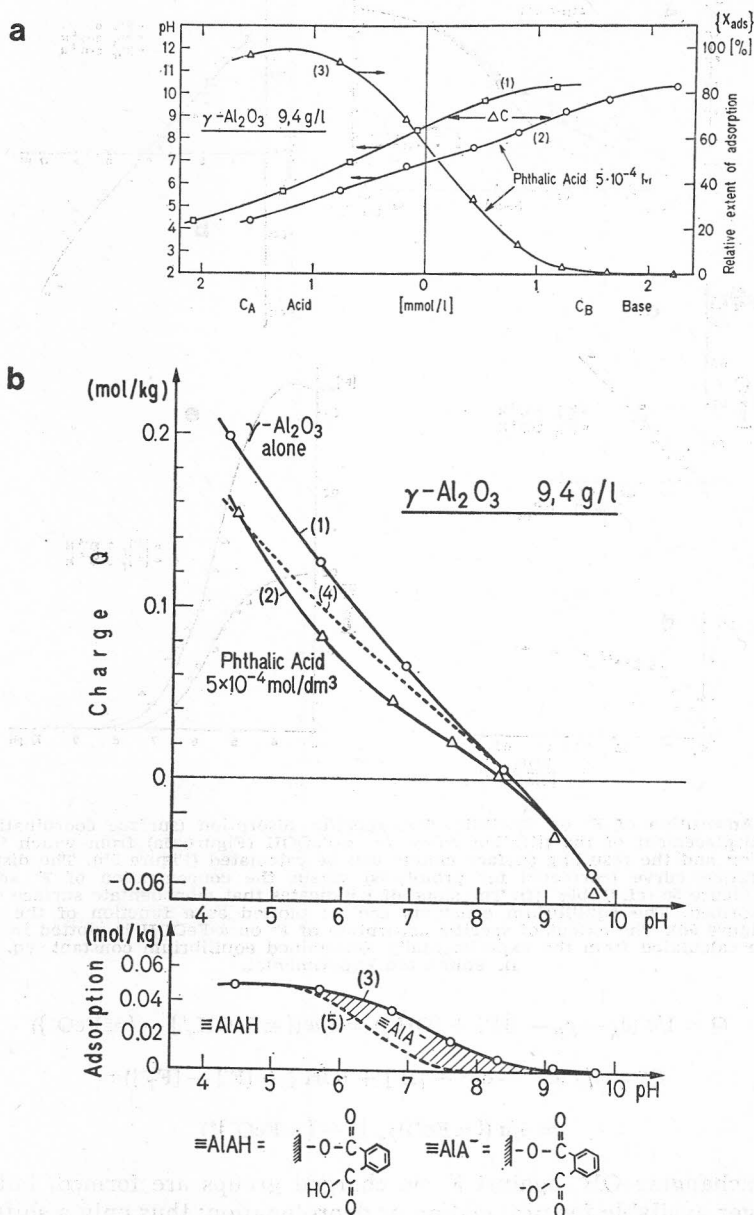


Figure 6. Adsorption of Phthalic Acid (H_2A) on $\gamma\text{-Al}_2\text{O}_3$ and its Effect on the Surface Charge. Displacement of the titration curve for $\gamma\text{-Al}_2\text{O}_3$ by adsorption of phthalic acid (Figure 6a) and the effect on the surface charge (Figure 6b). The charge vs pH curves (1) and (2) have been calculated from alkalimetric titration curves of Al_2O_3 in absence and presence of phthalic acid, respectively. The adsorption of total phthalic acid (formation of $\equiv\text{AlAH}$ and $\equiv\text{AlA}^-$) was determined analytically (curve (3)). Curve (4) was calculated with the equilibrium constant, assuming that uncharged $\equiv\text{AlAH}$ only is formed.

the surface species, because the various surface sites (edges, faces) may have slightly different surface energies. Figure 5e compares the calculated (using $\log K_1^s = -4.2$) and measured extent of F^- binding. Maximum adsorption is at $pH \approx 3.5$.

Surface Coordination of Phthalic Acid on γ - Al_2O_3 . Figure 6 from ref. 6 shows the effect of the presence of phthalic acid (H_2A) on the titration curve of γ - Al_2O_3 and its surface charge. The titration curve is displaced toward lower pH values. The extent of the shift results from (1) OH^- released as a consequence of the binding of HA (2) the base requirement of H_2A in solution, and (3) the possible deprotonation of $\equiv AlAH$ (cf. equations (19), (20), Table I). The surface coordination of phthalic acid causes a reduction in surface charge (Figure 6b). In the lower pH-range the charge reduction can be explained by considering that some of the protolyzable $\equiv AlOH$ groups have been replaced by $\equiv AlXH$, i. e., the fraction $\{\equiv AlOH_2^+\}/\{\equiv AlOH_T\}$ has decreased. In the higher pH range, above ca. $pH = 6$ $\equiv AlXH$ deprotonates to $\equiv AlX^-$. Figure 6b illustrates that a combined measurement of the charge and extent of adsorption can be used to predict the type of surface species present. Supplementary electrokinetic measurements are also of indicative value.

Some Limitations of the Equilibrium Model

The validity of the ligand exchange equilibrium model is somewhat limited by realizing (1) that the intrinsic equilibrium constants can often not be determined very accurately; (2) that the elucidations of the charge dependence on the equilibrium constants is often rendered very difficult; and (3) that the surface equilibrium is often attained very sluggishly and, at best, a metastable equilibrium is attained.

We have already pointed out that the surface sites at edges, corners and faces of the surface are most likely characterized by different surface energies. As with ion exchange equilibria in resins and clays, it is reasonable to expect that activity coefficients of surface species vary with the degree of loading. Furthermore the experimental determination of the total number of surface sites (exchange capacity $\{\equiv MeOH_T\}$) is difficult; different methods give different values, and depending on geometric considerations of the adsorbable species, not all surface sites become accessible.

The addition of new charged groups to the surface influences the acidity constants of the remaining surface OH -groups. The assumption made in Table III that the adsorption at a given pH does not affect the proportion of protonated to non-protonated surface groups is an oversimplification. On the other hand taking the whole adsorbed charge into account with regard to the acidity constants may overemphasize the charge effect. Probably for these reasons, difficulties were experienced in predicting quantitatively at low pH the SO_4^{2-} adsorption at goethite surfaces⁴.

Despite these limitations the experimentally determined »average« equilibrium constants can be used to predict, at least semiquantitatively, the extent of adsorption and the resulting surface charge as a function of pH for wide ranges of solution variables and surface area concentrations.

APPLICATIONS

Predicting the Extent of Adsorption and of Surface Charge as a Function of pH and Solution Variables

The pH dependence of adsorption of weak acids and anions can, with the help of the ligand exchange model, be readily explained by the pH dependence of the $\equiv \text{MeOH}$ group and the affinity of the structural metal ion on the surface, $\equiv \text{Me}$ for the ligand and the pH-dependence of the latter; i. e., the adsorption curve can be predicted qualitatively from the acid base equilibrium of the oxide and the anion. Figures 7 and 8 compare the extent of adsorption

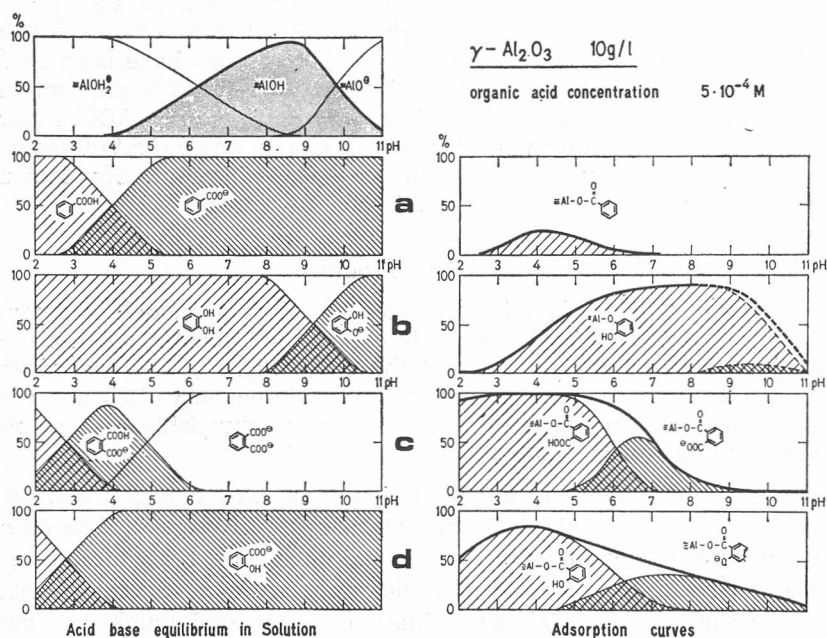


Figure 7. Extent of Adsorption of Aromatic Acids on $\gamma\text{-Al}_2\text{O}_3$ as a function of pH (right hand side) compared with the acid base properties of the reacting surface sites and of the solute ligands (left hand side). Curves have been calculated.

of ligands as a function of pH with the acid-base properties of the reactant surface sites and solute ligands. Often the pH of maximum adsorption occurs around $\text{pH} = \text{p}K_{\text{aH}_2\text{A}}$. This can be readily seen quantitatively by plotting in a double logarithmic plot the pH-dependence of the concentration of the species reacting in the surface coordination reaction, e. g., for the reaction $\equiv \text{MeOH} + \text{HA} \rightleftharpoons \equiv \text{MeA} + \text{H}_2\text{O}$:

$$\log \{ \equiv \text{MeA} \} = \log K_1^s + \log \{ \equiv \text{MeOH} \} + \log [\text{HA}] \quad (22)$$

As shown in Figure 9a extent of surface coordination can be readily predicted from such a diagram. If more than one surface complex is formed, the extent of adsorption is given by the sum of the individual surface species (Figure 9b).

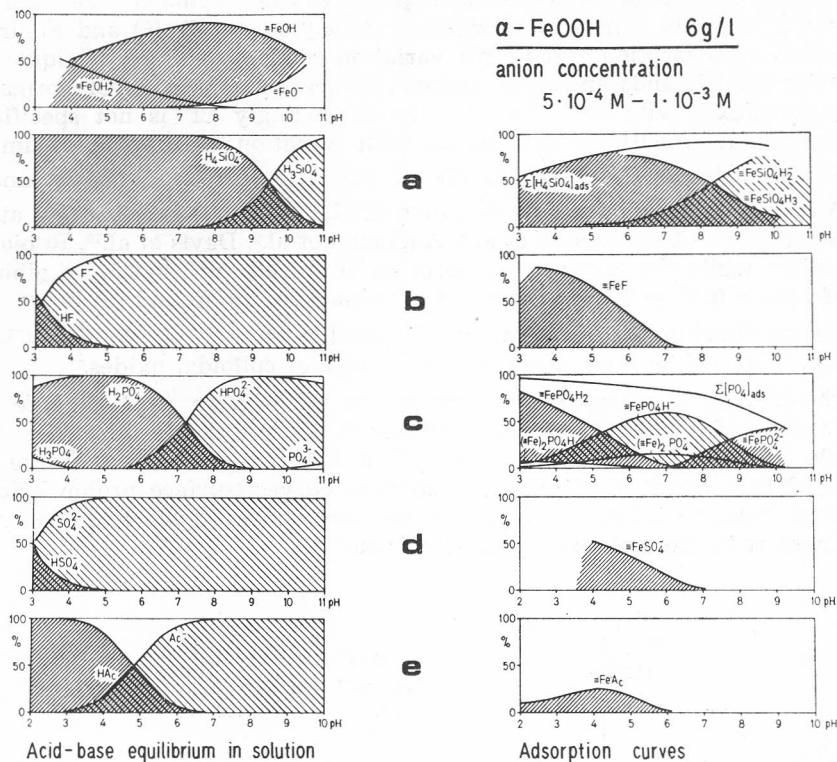


Figure 8. Extent of Adsorption of Anions and Their Conjugate Acids on $\alpha\text{-FeOOH}$ as a function of pH (right hand side) compared with the acid-base properties of the solute ligands and the reacting surface sites.

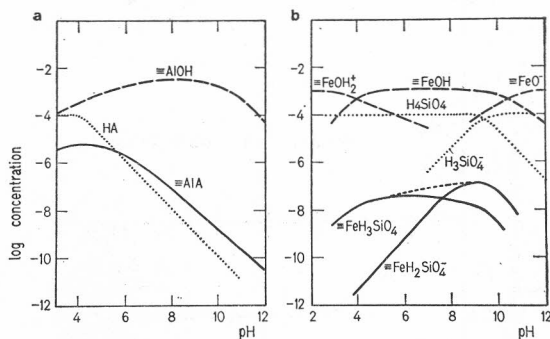


Figure 9. Prediction of the Extent of Surface Coordination. For the monoprotic acid HA (e. g. benzoic acid), Eq. (22) is plotted as a function of pH (Figure 9a). For silicic acid, two surface complexes can be formed (Figure 9b).

Because the surface equilibrium constant can be estimated from the corresponding stability constants in solution (cf. equations (8), (9) and Figure 3), the extent of adsorption and its pH variation can be predicted semiquantitatively for most ligands and most hydrous oxides. For example, Cl^- forms less stable complexes with Fe^{3+} than F^- . Correspondingly Cl^- is not specifically adsorbed on $\alpha\text{-FeOOH}$. In accordance with Equation 22, the maximum adsorption of selenite ($\text{p}K_{\text{H}_2\text{SeO}_3} = 2.35$), of arsenate ($\text{p}K_{\text{H}_2\text{AsO}_4} = 2.25$) and of EDTA ($\text{p}K_{\text{H}_4\text{Y}} \approx 2$) on iron(III) oxide (hydroxide) or Al(III) oxide occurs at low pH values (pH 1–3) (Hingston et al.⁸, Anderson et al.⁹, Davis et al.¹⁰, Rubio and Matijević¹¹, while the maximum adsorption of silicate ($\text{p}K_1 = 9.5$) on gibbsite⁸ and of borate ($\text{p}K_1 = 9.1$) on activated alumina¹² occurs around pH = 9.

The equilibrium constants can also be used to estimate the *Surface Charge* (eq. (12), (13)) and to predict the stability range of colloidal oxides.

The binding of phosphate to hydrous oxides, e. g. on Al_2O_3 and FeOOH , is characterized by a proton release and a shift of iep to lower pH values. With goethite ($\alpha\text{-FeOOH}$) dispersed in phosphate solutions, the fixed charge was computed as a function of pH from titration curves (surface proton balance) and from analytic information (phosphate adsorbed)⁴ (Figure 10). Reasonable agreement with electrokinetic data is obtained.

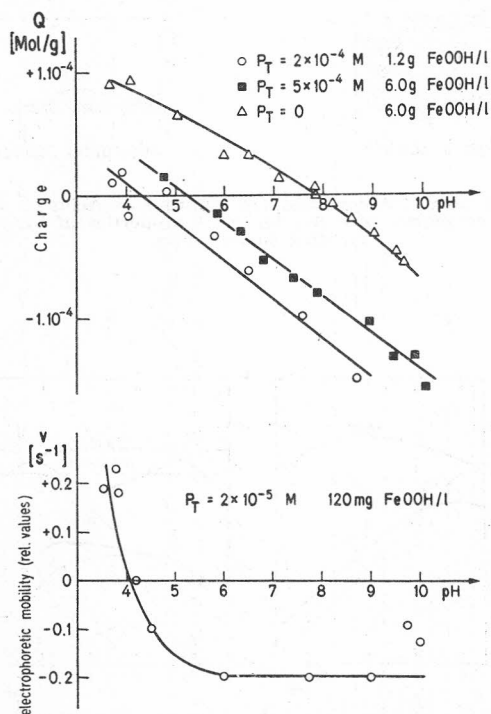


Figure 10. Effect of Adsorption of Phosphate on Goethite upon its Surface Charge. The fixed charge is computed from alkalimetric titration curves and from analytical determination of the quantity of P_T adsorbed. For the electrophoretic mobility measurement (Figure b), a ratio of P_T/FeOOH equal to that of the lower charge vs pH curve (Figure a) was used (Equilibrium values of P_T in solution are approximately the same).

Predicting Domains of Colloid Stability

With the help of the equilibrium constants iep-values can be calculated for various values of pH and solute concentrations. In a colloid stability domain diagram (Figure 11) an isoelectric line can be computed; in the immediate proximity of this line the oxide dispersion is uncharged. Colloid stability is assumed to occur on either side of the line beyond positive and negative threshold charges. Figure 11 shows the pH- $\log P_T$ ranges in which goethite is col-

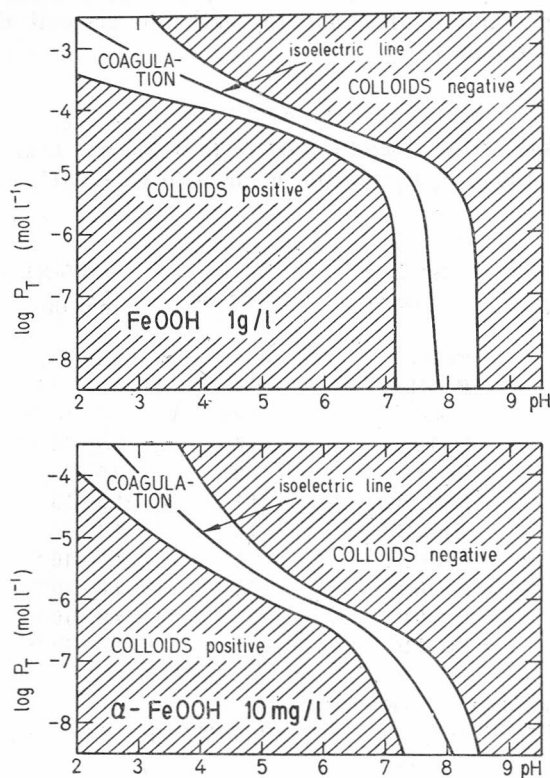


Figure 11. Calculated Colloid Stability of α -FeOOH in Presence of Phosphate. $\log P_T$ vs PH Domain of Colloid Stability of Goethite Dispersions. These domains have been calculated with the help of equilibrium constants (Table I) and using corrections for coulombic attraction or repulsion. Rapid coagulation should occur in the proximity of the isoelectric line. Colloid stability is assumed to occur at positive and negative charges corresponding to a zeta potential of 30 mV.

loidchemically stable as negatively or positively charged colloids. The computed diagram is similar to a diagram for the α -Fe₂O₃-phosphate system experimentally determined by Breeuwsma and Lyklema¹³.

Implications for Natural Waters

A set of surface equilibrium constants permits the estimation of the surface speciation of an oxide in a natural water of a given composition.

Table IV gives the calculated surface speciation and surface charge for goethite equilibrated with the inorganic components of a fresh water lake^{4,5}. The simultaneous equilibria have been resolved with an iterative computer program that considers the charge dependence of the equilibrium constants. Table IV shows that the surface sites of α -FeOOH will be preponderantly occupied by phosphate and silicate although these species are present in very small concentrations in the water. These species will also to a large extent determine the negative surface charge of α -FeOOH at the pH of the natural water. A more realistic model of a natural water has also to consider the adsorption of organic matter¹⁴ and might have to take into account the formation of ternary surface complexes^{1,21}.

TABLE IV

Speciation of the Goethite Surface in a Natural Lake Water
 $\{\equiv\text{FeOH}\}_T = 1.10 \cdot 10^{-6} \text{ mol/dm}^3 (= 1.10 \cdot 10^{-3} \text{ g/dm}^3 \text{ with } \{\equiv\text{FeOH}\}_T = 1.10 \cdot 10^{-3} \text{ mol/g})$

pH = 7,5

X	$\frac{C_T}{\text{mol dm}^{-3}}$	Surface species	$\log K_{\text{intr.}}$	$\frac{[\equiv\text{FeX}]}{\text{mol dm}^{-3}}$	$\frac{\%}{[\equiv\text{FeOOH}]_T}$
—	—	=FeOH	—	$2.5 \cdot 10^{-7}$	25
H ⁺	$3.2 \cdot 10^{-8}$	=FeOH ₂ ⁺	—6.4	$1.6 \cdot 10^{-7}$	16
OH ⁻	$4.9 \cdot 10^{-7}$	=FeO ⁻	—9.25	$5.5 \cdot 10^{-10}$	0.05
SO ₄ ²⁻	$1.10 \cdot 10^{-4}$	=FeSO ₄ ⁻	—5.8	$1.0 \cdot 10^{-11}$	$1 \cdot 10^{-3}$
H ₂ PO ₄ ⁻	$1.10 \cdot 10^{-6}$	=FeHPO ₄ ⁻	7.2	$3.5 \cdot 10^{-7}$	35
H ₄ SiO ₄	$5.10 \cdot 10^{-5}$	=FeH ₃ SiO ₄ ⁻	4.1	$1.5 \cdot 10^{-7}$	15
		=FeH ₂ SiO ₄ ⁻	—3.3	$2.4 \cdot 10^{-8}$	2.4
HCO ₃ ⁻	$5.10 \cdot 10^{-3}$	=FeCO ₃ ⁻	2.5	$4.9 \cdot 10^{-8}$	4.9
Mg ²⁺	$2.10 \cdot 10^{-4}$	=FeOMg	—6.2	$7.8 \cdot 10^{-9}$	0.8
Ca ²⁺	$1.10 \cdot 10^{-3}$	=FeOCa ⁺	—8	$4.9 \cdot 10^{-10}$	0.05
Pb ²⁺	$1.10 \cdot 10^{-8}$	=FeOPb ⁺	—3	$4.9 \cdot 10^{-10}$	0.05

$Q \approx -2.5 \cdot 10^{-7} \text{ mol/dm}^3 \approx -5.10 \cdot 10^{-5} \text{ mol/g}$.

The constants for HCO₃⁻, Ca²⁺ and Pb²⁺ are estimated.

Organic matter which has been desorbed from lake sediments¹⁴ shows similar adsorption behaviour on alumina as phthalic and salicylic acid (Figure 12). On the basis of the equilibrium constants for organic acids on γ -Al₂O₃ (Table I), we estimate that, in the concentration range of organic acids of $1\text{--}3 \cdot 10^{-5} \text{ mol dm}^{-3}$, ca. 10% of the surface sites may be occupied by bound organic acids. This fraction may however be higher in nature because soluble polar organic substances are present in polymeric form¹⁴. The results of the calculations illustrate that oxides or oxide hydroxides of Fe(III) are an important sink and regulating factor for phosphate and silicate.

SURFACE COMPLEXATION AND THE ELECTRIC DOUBLE LAYER

In the ligand exchange model discussed here, the interaction of solutes with the oxide surface is seen primarily as a chemical process the equilibria of which can be expressed with mass law and material balance equations. How-

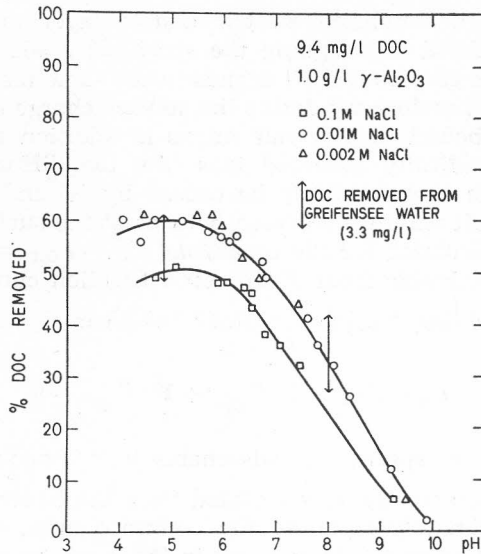


Figure 12. Adsorption Curves of »Fulvic Acids« on γ -Aluminium Oxide, Measured as Dissolved Organic Carbon (DOC) Removed at 22 °C (From J. Davis¹⁴). The fulvic acids were collected from Swiss lake sediments by desorption at high pH. In another experiment, the adsorption of DOC from a natural lake water (Greifensee water) was measured at two different pH.

ever, the correction of the equilibrium constants to intrinsic ones and the evaluation of the surface charge implies a certain description of the electric double layer. In Figure 13 we juxtapose the thermodynamic model of the

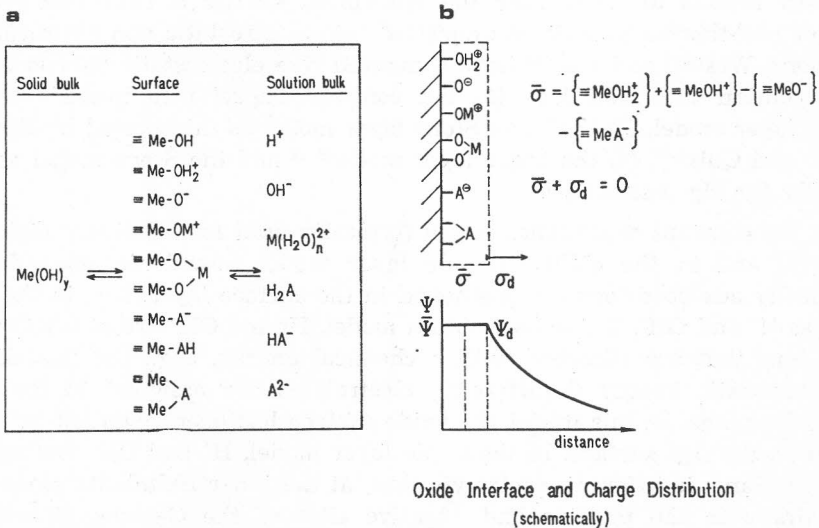


Figure 13. Schematic Representation for the Interactions of M^{2+} and H_2A or its Bases at a Hydrated Oxide Interface.

- a) Thermodynamic model: the surface is treated as a separate metastable phase,
- b) electric double layer model with corresponding potentials (σ : surface charge; σ_d : charge in the diffuse layer.)

oxide surface with a simplified electric double layer model. As explained before, we feel justified in assigning the specifically adsorbed surface-, i. e., »inner sphere« »type coordinated — ligands in the same mean plane of adsorption« as $\equiv \text{MeOH}$. Therefore we define the surface charge σ_0 to include all the charges caused by bound cations and anions in addition to H^+ and OH^- and consign all non-specifically adsorbed ions into the diffuse layer. Since the *zero point of charge* is defined¹⁵ to be caused by H^+ and OH^- only, the zpc corresponds to the pH where the proton balance at the surface, $\Gamma_{\text{H}} - \Gamma_{\text{OH}} = 0$, is zero; it can be calculated for the conditions $\Gamma_{\text{H}} - \Gamma_{\text{OH}^-} = 0$ (cf. equation 13) which is readily obtainable from alkalimetric titration curves.

The *isoelectric point*, iep, on the other hand corresponds to the condition where

$$\Gamma_{\text{H}} - \Gamma_{\text{OH}} + \sum_i z \Gamma_{\text{M}_i^{z+}} - \sum_i z \Gamma_{\text{A}_i^{z-}} = 0 \quad (23)$$

Only in the absence of specifically adsorbable ions is $\text{zpc} = \text{iep}$.

The electrokinetic charge, as calculated from the electrokinetic potential ζ may be set approximately equal to the diffuse charge; thus it reflects the surface charge (plus, in principle any ions in the Stern layer not yet accounted for in the fixed surface charge). If $\zeta = 0$, then $\text{pH} \approx \text{pH}_{\text{iep}}$.

Other Models for the Oxide-Water Interface

Various authors have described various models to account for the specific adsorption of ions on hydrous oxide surfaces (James, Healy^{16,17}, Quirk et al.^{8,18}, Anderson et al.⁹ Lyklema¹⁹, Davis and Leckie²¹, Stumm²², Schindler²³).

Most models differ in how the adsorption energy is separated (on the basis of non-thermodynamic assumptions) into electrostatic and chemical contributions. Westall and Hohl²⁴ have compared five electrostatic models for the oxide-solution interface, i. e., (1) the constant capacitance model^{1,2} (2) the diffuse layer model, (3) the basic Stern layer model as interpreted by Bowden, Posner and Quirk¹⁸, (4) the triple layer model^{20,21} and the Stern model as used typically for Hg (surfaces)²⁵.

In the constant capacitance model (typically used for relatively high ionic strength) and in the diffuse double layer model (low ionic strength), the specifically adsorbed ions are positioned in the surface layer, i. e., in the same plane as H^+ and OH^- . In the basic Stern model, H^+ and OH^- are at the O-plane, while ions that are adsorbed with a chemical energy, e. g., the ligands, and an electrostatic energy (indifferent), electrolytes are assigned to the inner Helmholtz plane. In this model the oxide surface has been regarded as being similar to the AgI surface. In the triple layer model, H^+ and OH^- are again at the zero plane; indifferent electrolyte ions, at the inner Helmholtz plane form ion pairs with the positive and negative sites of the O-plane. Specifically adsorbed ions are also assigned to the inner Helmholtz plane. Finally, in the Stern layer, as used typically on Hg surfaces, H^+ and OH^- , as well as specifically adsorbable and electrostatically adsorbable electrolytes are at the inner Helmholtz plane.

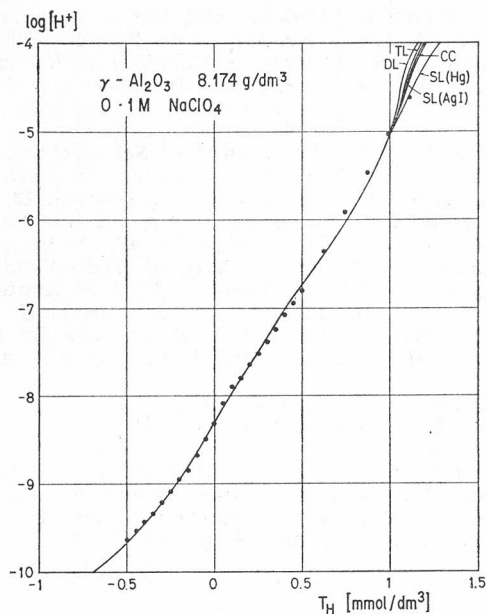


Figure 14. Comparison of the Calculations of the Titration Curves of γ - Al_2O_3 with five Different Electrostatic Models (from J. Westall and H. Hohl²⁴).

Figure 14 (from Westall and Hohl²⁴) compares these five models representing the acid/base titration of γ - Al_2O_3 in 0.1 M NaClO_4 . With a least square method the parameters that fitted the model best to experimental data were calculated [Westall, Hohl²⁴]. As this Figure illustrates all models represent the experimental data equally well although the values of corresponding parameters in different models are not the same.

Thus, all the models may be viewed as being of the correct mathematical forms to represent the data but are not necessarily an accurate physical description at the interface. In other words, all models can be used to describe experimental data over the range of experimental data; the »intelligence« of the data, on the other hand is not sufficient to gain insight into the physical nature of the interface. The problem of separating the chemical and electrostatic energy is experimentally indeterminate for oxide-water interfaces.

Acknowledgments. — Valuable advice given by Herbert Hohl, Walter Schneider and John Westall is acknowledged. This research has been supported in part by the Swiss National Foundation and by the Swiss Department of Commerce (Commission of the European Communities, Project COST 64b).

REFERENCES

1. P. W. Schindler, in: M. A. Anderson and A. Rubin, (Eds.), *Ann. Arbor Science*, Mich., to be published.
2. W. Stumm, H. Hohl, and F. Dalang, *Interaction of Metal Ions with Hydrous Oxide Surfaces*, *Croat. Chem. Acta* **48** (1976) 491.
3. W. Stumm and J. J. Morgan, *Aquatic Chemistry*, Wiley-Interscience, New York 1970.
4. L. Sigg, *Ph. D. Thesis Nr. 6417*, ETH, Zürich 1979.

5. L. Sigg and W. Stumm, *Colloids and Surfaces*, to be published.
6. R. Kummert, *Ph. D. Thesis Nr. 6371*, ETH Zürich 1979.
7. R. Kummert and W. Stumm, *J. Colloid Interface Sci.* **75** (1980) 373.
8. F. J. Hingston, A. M. Posner, and J. P. Quirk, *J. Soil Sci.* **23** (1972) 177.
9. M. A. Anderson, J. F. Ferguson, and J. Gawis, *J. Colloid Interface Sci.* **54** (1976) 391.
10. J. A. Davis and J. O. Leckie, *Environm. Sci. Technol.* **12** (1978) 1309.
11. J. Rubio and E. Matijević, *J. Colloid Interface Sci.* **68** (1979) 408.
12. W. Choi and K. Y. Chen, *Environm. Sci. Technol.* **13**, (1979) 189.
13. A. Breeuwsma and J. Lyklema, *J. Colloid Interface Sci.* **43** (1973) 437.
14. J. Davis, *EAWAG, Contaminants and Sediments*, to be published.
15. J. Lyklema, *Interfacial Electrochemistry of Hydrophobic Colloids*, in: E. D. Goldberg, (Ed.), *The Nature of Seawater* Dahlem Konferenzen, Berlin 1975.
16. R. O. James and T. W. Healy, *J. Colloid Interface Sci.* **40** (1972) 42, 53, 65.
17. D. E. Yates and T. W. Healy, *J. Colloid Interface Sci.* **52** (1975) 222.
18. J. W. Bowden, A. M. Posner, and J. P. Quirk, *Austr. J. Soil Res.* **15** (1977) 121.
19. J. Lyklema, *Croat. Chem. Acta* **43** (1971) 249.
20. D. E. Yates, S. Levine, and T. W. Healy, *Trans. Faraday Soc.* **70** (1974) 1807.
21. J. A. Davis and J. O. Leckie, *J. Colloid Interface Sci.* **63** (1978) 480, and in: E. A. Jenne, (Ed.), *Chemical Modeling — Speciation, Sorption, Solubility and Kinetics in Aqueous Systems*, ACS Symposium Series **93**, Chap. 15 (1979).
22. W. Stumm, C. P. Huang, and S. R. Jenkins, *Croat. Chem. Acta* **42** (1970) 223.
23. P. W. Schindler, B. Fürst, R. Dick and P. Wolf, *J. Colloid Interface Sci.* **55** (1976) 469.
24. J. Westall and H. Hohl, *Advan. Colloid Interface Sci.* **12** (1980) 265.
25. O. Stern, *Z. Elektrochem* **30** (1924). 508.

SAŽETAK

Model ligandne izmjene za adsorpciju anorganskih i organskih liganada na površinama hidratiziranih oksida

W. Stumm, R. Kummert i L. Sigg

Preložen je model kojim se adsorpcija slabih kiselina i nekih aniona na površinama hidratiziranih oksida može promatrati kao reakcija izmjene liganada. Model predpostavlja izravnu vezu liganada i površine, a adsorbirana količina i njezina ovisnost o pH medija zavisi o afinitetu aktivnih mjesta površine za ligande. Na primjerima određivanja kiselosti α -FeOOH, koordinacije iona F^- na α -FeOOH, te za koordinaciju ftalne kiseline na γ - Al_2O_3 , pokazano je eksperimentalno određivanje konstanti ravnoteže adsorpcije. Adsorpcija slabih kiselina najjača je kod $pH = pK$, a konstante ravnoteže za stvaranje površinskih kompleksa pokazuju iste trendove kao i one za topljive vrste. Na taj su način moguća pretkazivanja površinskih stanja na osnovi poznavanja stanja u otopini.

Ograničenja primjenljivosti modela očituju se u činjenici da se (a) intrinzične konstante stabilnosti ne mogu odrediti dovoljno točno, (b) da je vrlo teško odrediti ovisnost konstante ravnoteže površinskog kompleksa o naboju površine, i (c) da se ravnoteža na površini obično uspostavlja vrlo sporo i da je često prekrivena metastabilnim stanjima. Osim toga su zbog efekta rubova ploha ili defekata površine često karakterizirane različitim raspodjelama energijskih stanja mjesta adsorpcije, te različite metode daju različite podatke.